COMMUNICATION

Detection of Western Diamondback Rattlesnake (*C. atrox*) venom using Glycopolymer Functionalised Gold Nanoparticles

Mahdi Hezwani,[a†] Derecash Anokye,[a†] Douglas E. Soutar,[a] Melissa Ligorio,[a] Neil Prabhakar,[a] Alexander Cantor,[a] Roberto Terracciano,[a] Marc Walker[b] and Alexander N. Baker*[a]

[a] Department of Chemistry, University of Warwick, Gibbet Hill Road, CV4 7AL, Coventry, UK

[b] Department of Physics, University of Warwick, Gibbet Hill Road, CV4 7AL, Coventry, UK

Every 5 minutes, 50 people are bitten by a snake worldwide, four will be permanently disabled and one will die.[1,2] Most approaches to treating and diagnosing snake envenomation rely on antibody-based solutions. Here, we present a proof-of-concept for a glycan-based UV-vis assay to detect *Crotalus atrox* (*C. atrox*) venom versus model proteins and Indian Cobra (*Naja naja*, *N. naja*) venom.

Snake envenomation is a neglected tropical disease (NTD) requiring urgent attention. The current treatment for snake envenomation utilises antibody-based antivenoms. Monovalent antivenom (which targets a single venom) treatment is best practice; however, using a monovalent antivenom requires the identification of snake species, as a wrong prescription will be less effective and may have serious consequences.[3,4] While a polyvalent antivenom can be used, it has adverse patient outcomes and greater risk of side-effects.[4] Identifying envenomation and the snake species responsible for the bite injury is, therefore, vital to improving patient outcomes within the golden window.[5,6] Current research has focused on antibody-based solutions, both in diagnostics and treatments. However, few robust, low-cost and commercially available point-of-care diagnostics are available for snake envenomation.[6]

Observational, qualitative approaches for diagnosis can lead to poor patient outcomes and the injudicious prescribing of inappropriate pharmaceuticals. In snake envenomation, observational approaches rely on bite configuration, knowledge of snake species in the vicinity, talking to witnesses and clinical manifestations. However, many toxins in snake venoms exhibit similar physiochemical and pharmacological properties and, therefore, similar clinical responses. Furthermore, envenomation from the same snake species but from a different geographical location have been shown to have variations in the venom composition.[7] Even when the snake is present for identification, there is a chance of misidentification, which can lead to complications in administering antivenoms.[8] Therefore, rapid, low-cost empirical diagnostics that are usable at the point-of-care (POC) are needed, especially for snake bite victims who are time-critical patients often treated by traditional healers.[9] There is a pressing need for this technology with the WHO estimating that snake envenomation (bites) cause ~100,000 deaths a year and approximately three times as many amputations and permanent disabilities. This is believed to be under-estimate due to a lack of robust reporting.[10–12]

Glycoconjugates, carbohydrates/glycans covalently linked to other chemical species such as proteins, peptides, lipids etc., are fundamental to the normal functioning of organisms,[13] while their inhibition or manipulation can be detrimental,[14,15] or even fatal.[16–18] They perform a vast range of roles, including cell signalling,[19] hormonal action,[20] cancer progression,[21] embryonic development,[22] correct protein folding/structure[23,24] and mediating immune responses/infection.[25,26] Glycans can also be chemically synthesised, so there is no need to raise antibodies, and the sheer range of tools to alter glycan presentation make them appealing targets. Consequently, there is a significant opportunity to target glycans to differentiate glycoforms, or their lectins ("glycan-readers"), for diagnosis.[27–30]

Lectins are a broad family of glycan-binding proteins that are neither enzymes, transporters or antibodies. They often have highly conserved carbohydrate-binding domains.[31,32] Examples of lectins include the Shiga toxin,[33] cholera toxin[34] and ricin,[35] while also being found in snake venoms.[36] Notably, the use of lectins for staining histology samples has been established for decades to identify diseased tissue based on glycosylation.[31] In a histological study, the binding of glycans to snake venoms was first reported in *Bothrops atrox* (fer-de-lance, a pit viper) venom.[37] While other snake venom lectins have been studied, for example *C. atrox* (western diamondback rattlesnake) venom (one of the few commercially available venoms with glycan array data),[38] many *Viperidae* venoms lack in-depth glycan studies despite constituting up to 10% of venom components in the *Viperidae* family of over 200 snake species.[39] The incorporation of glycans into assays for snake bite has not been widely explored.

Plasmonic gold nanoparticles (and other metals[40]) are important in colorimetric aggregation assays, a valuable diagnostic technique. Mirkin *et al.* showed that gold nanoparticles

*Corresponding Author: alexander.baker@warwick.ac.uk

functionalised with complementary DNA strand aggregate produced a colour shift from red (dispersed) to blue (aggregated). While Georgiou *et al.* demonstrated the use of glycan-functionalised nanoparticles for the detection of SARS-COV-2 spike protein, and Richards *et al.* for detecting influenza hemagglutinins.[41,42] This occurs due to the coupling of surface plasmon resonance (SPR) bands, which are measurable by UV-vis spectroscopy and often observable by eye.

Herein, we report the design and synthesis of an initial proof-of-concept for a glycopolymer functionalised gold nanoparticle-based UV-vis assay for the detection of *C. atrox* venom.

Our system consists of gold nanoparticles functionalised with glycans on a polymer tether. The polymeric tether, Poly(*N*-hydroxyethyl acrylamide) (pHEA), was synthesised by thermally initiated reversible addition-fragmentation chain transfer (RAFT) polymerisation, using 2-(dodecylthiocarbonothioylthio)-2-methylpropionic acid pentafluorophenyl ester (PFP-DMP) as the RAFT agent, following methodologies previously described by Micallef *et al.*[43] This produced polymers with predictable chain length and low dispersity. The RAFT agent and polymers were characterised by SEC, mass spectrometry, FTIR, and ^{1}H, ^{13}C and ^{19}F NMR (Table 1.). A RAFT agent with an activated ester as the R group was chosen to allow for facile installation of an amino-glycan at the α-chain end of polymers.

Polymer	[CTA]:[M]	Conversion, %	Mn SEC (g.mol^{-1})[b]	Mn nmr (g.mol^{-1})[c]	DP[b]	$Đ_M$[b]
$pHEA_{52}$	1:40	98	6530	7050	52	1.35
$pHEA_{42}$	1:30	98	5370	6190	42	1.20
$PHEA_{25}$	1:20	98	3430	4100	25	1.11

Table 1 – Synthesised polymer. [a] Molar ratio of chain transfer agent (CTA) to monomer; [b] Determined by SEC in DMF with 5 mM NH_4BF_4 eluant, calibrated with poly(methyl methacrylate) standards. [c] Determined from ^{1}H NMR end-group analysis.

Rattlesnake venom lectin (RSVL) in *C. atrox* venom has known affinity toward *N*-acetyl-galactosamine, galactose and lactose (a disaccharide with a terminal galactose) residues.[38] While SBA and WGA were chosen as control lectins. SBA has known affinity to α/β-*N*-acetyl-galactosamine and, to a lesser extent, galactose residues.[44] Glucose has known affinity to WGA, and mannose has affinity to a range of lectins including the mannose-binding lectin (MBL), which is key to many biological processes and toward the C-type lectin found in the venom of *Oxyuranus scutellatus* (Australian coastal taipan snake).[45–47]

Six amino-glycans were therefore substituted for the activated ester at the α-terminus of the polymer. 2-deoxy-2-amino-glucose (glucosamine) (Glc-2), 2-deoxy-2-amino-mannose (mannosamine) (Man-2) and 2-deoxy-2-amino-galactose (galactosamine) (Gal-2) were purchased from commercial suppliers, while 1-amino-1-deoxy-lactose (Lac-1), 1-amino-1-deoxy-*N*-acetyl-galactosamine (GalNAc-1) and 1-amino-1-deoxy-galactose (Gal-1) were synthesized. Two synthetic methods were employed to achieve amine functionalisation at the anomeric position of lactose, galactose and *N*-acetyl-galactosamine. The first was a two-step method using 2-azido-1-3-dimethylimidazolinium hexafluorophosphate (ADMP) to substitute the anomeric hydroxyl for an azide before using a Pd/C catalyst to reduce the azide to an amine.[29] The second utilised ammonium bicarbonate and ammonia to substitute the anomeric hydroxyl directly to an amine on both galactose and lactose.[48,49] Products of both methods were analysed by mass-spectrometry and FTIR to observe the loss of hydroxyl and gain of amine groups. Comparing the two synthetic methods, the literature suggested that using ADMP in the former synthetic method results in a controlled set of amino-glycan anomers.[50] This is important as lectins found in certain snake venoms, such as *Croatalus ruber (C. ruber),* displayed β-galactoside anomeric specificity over the α-anomer.[51] Additionally, a study by *Young et al.* has shown that *C. atrox* has displayed specificity toward α-Gal and α-GalNAc non reducing termini, however there is currently little evidence if this trend is consistent with other glycans.[38]

For the first round of testing, the six aminoglycans were added to $pHEA_{42}$ before immobilisation onto gold nanoparticles synthesised by a seeded growth mechanism (16 nm) or purchased (40 nm).[52] This produced a library of twelve glycosylated nanoparticles, which were characterized by dynamic light scattering (DLS), transmission electron microscopy (TEM), UV-vis spectroscopy (UV-vis) and x-ray photoelectron spectroscopy (XPS) (Figure 1.).

Elemental analysis using XPS was conducted on dried particles to determine their surface composition, which confirmed polymer on the gold surface due to the presence of an N 1*s* peak - nitrogen is not present in naked AuNP samples or background. Furthermore, the presence of amide (C(O)NC) and amine (C(O)NC) peaks in the C 1*s* (Figure 1D), and in the N 1*s* scans (amine and amides have similar/overlapping binding energies so were not distinguishable), showed the presence of PHEA.

In one system, partial or full aggregation of glycosylated nanoparticles was observed by eye (a noticeable change from deep red to a blue/purple or colourless). Aggregation was confirmed by UV-Vis and DLS prior to the plasmonic assay testing, indicating a colloidally unstable system, hence unsuitable for this study and removed from all further testing (Lac-1-$pHEA_{42}$@$AuNP_{40}$). In this case, the polymer chain may not have been able to provide colloidal stability for the larger molecular weight lactose disaccharide and the larger 40nm particle. The literature has discussed this phenomenon before with similar systems and is further supported as Lac-1-$pHEA_{42}$@$AuNP_{16}$ was stable.[43]

To determine the stability of each permutation of $AuNP_x$ and $pHEA_x$ a UV-vis assay was undertaken in triplicate using a fixed OD_{MAX}(SPR) of 0.5 of each AuNP system and varying concentration of SBA, WGA (1, 0.5, 0.25, 0.125, 0.0625, 0.03125, 0.0156 mg.mL^{-1}) and *C. atrox* venom (8, 6, 4, 2, 1, 0.5, 0.25, 0.125, 0.0625, 0.03125, 0.0156 mg.mL^{-1}) to determine the sensitivity and specificity of each system. Absorbance was measured following incubation at room temperature (~20 ℃) for 20 minutes. The *C. atrox* venom, while a real-world target, is known to contain a variety of proteins, including RSVL, a C-type lectin in a relatively low quantity (1-2%), whereas the SBA and WGA are pure lectins.[38,53] Hence a higher concentration of the venom was used. All absorbances were normalised at OD_{450} to allow for direct comparison.

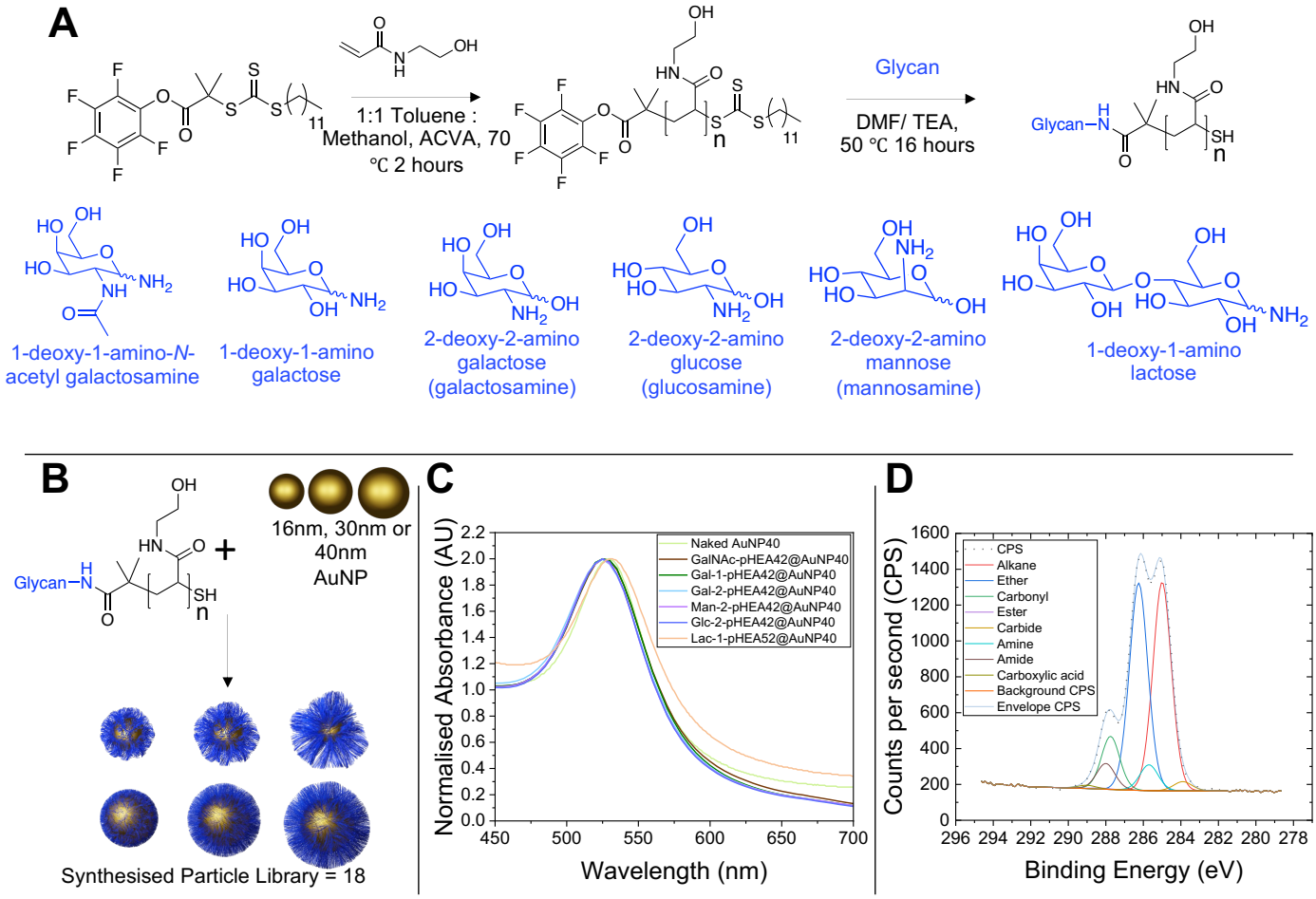

E

GalNAc-pHEA$_{42}$@AuNP$_{16}$	GalNAc-pHEA$_{42}$@AuNP$_{40}$	Gal-1-pHEA$_{42}$@AuNP$_{16}$	Gal-1-pHEA$_{42}$@AuNP$_{40}$
Gal-2-pHEA$_{25}$@AuNP$_{16}$	Gal-2-pHEA$_{42}$@AuNP$_{16}$	Gal-2-pHEA$_{25}$@AuNP$_{30}$	Gal-2-pHEA$_{42}$@AuNP$_{30}$
Gal-2-pHEA$_{42}$@AuNP$_{40}$	Glc-2-pHEA$_{25}$@AuNP$_{16}$	Glc-2-pHEA$_{42}$@AuNP$_{16}$	Man-2-pHEA$_{42}$@AuNP$_{16}$
Man-2-pHEA$_{42}$@AuNP$_{40}$	Lac-1-pHEA$_{25}$@AuNP$_{16}$	Lac-1-pHEA$_{42}$@AuNP$_{16}$	Lac-1-pHEA$_{25}$@AuNP$_{30}$
Lac-1-pHEA$_{42}$@AuNP$_{30}$	Lac-1-pHEA$_{42}$@AuNP$_{40}$	Lac-1-pHEA$_{52}$@AuNP$_{40}$	

Figure 1. – Synthesis of gold nanoparticle library with glycan terminated polymer tethers and analysis A) Polymerisation of *N*-hydroxyethyl acrylamide synthesis by RAFT, followed by displacement of the PFP ester with amino-glycans, B) gold nanoparticle functionalisation with glycopolymer, C) Representative UV-vis spectra of (40 nm) nanoparticle systems, D) C 1*s* x-ray photoelectron spectrum of Gal-2-PHEA$_{42}$@AuNP$_{40}$ and E) written representation of all synthesised nanoparticles.

After running the plasmonic assays, partial/full non-specific aggregation was observed for several systems which displayed colloidal instability, including GalNAc-pHEA$_{42}$@AuNP$_{40}$ and Gal-1-pHEA$_{42}$@AuNP$_{40}$, so were excluded from further studies as to not provide any false-positives. Strong binding is indicated by variations seen at Abs$_{700}$ and/or SPR bands coupling with a shift/drop at UV$_{MAX}$ in the UV-Vis spectra. This was observed in one or both of the control lectins with various systems; Glc-2-pHEA$_{42}$@AuNP$_{40}$ bound to SBA and WGA strongly, Gal-1-pHEA$_{42}$@AuNP$_{16}$ and Gal-2-pHEA$_{42}$@AuNP$_{16}$ bound to WGA strongly, and Man-2- pHEA$_{42}$@AuNP$_{16}$ bound to WGA and SBA moderately, with previous literature supporting these results.[45,53–60] Since these systems showed no binding to the *C. atrox* venom, these were removed from all future testing. Furthermore, Glc-2-pHEA$_{42}$@AuNP$_{16}$ and GalNAc-1-pHEA$_{42}$@AuNP$_{16}$ displayed little to no affinity toward any of the lectins, so were also excluded from future testing, while Man-2-pHEA$_{42}$@AuNP$_{16}$ aggregated with *C. Atrox* venom, along with both WGA and SBA, indicating non-specific binding.

From the initial round of testing, two systems displayed promise: Lac-1-pHEA$_{42}$@AuNP$_{16}$ and Gal-2-pHEA$_{42}$@AuNP$_{40}$. Both displayed strong binding toward the *C. Atrox* venom, with the former displaying some affinity toward the SBA and WGA and the latter displaying little affinity toward SBA and some affinity toward WGA. The affinity for both systems toward *C. atrox*, SBA and WGA was expected, as Gal residues have been reported to be specific for RSVL.[38,61] These systems were therefore studied further, tuning polymer length and AuNP size.

Gal-2-pHEA$_{42}$@AuNP$_{40}$ demonstrated an approximate limit of detection (LoD) to *C. atrox* versus the WGA and SBA controls at 15 µg/ml and 20 µg/ml respectively (Figure 2.). This is the point at which *C. atrox* binding cannot be discerned above the binding of WGA and SBA. Comparing this LoD to conventional diagnostic tools to detect snake venoms shows promise Lión *et al.* developed a latex agglutination test to detect *Crotalus spp.* venoms with a LoD of 167 µg/mL, with an assay duration of 10 minutes, which is comparable to the aims of this study.[62]

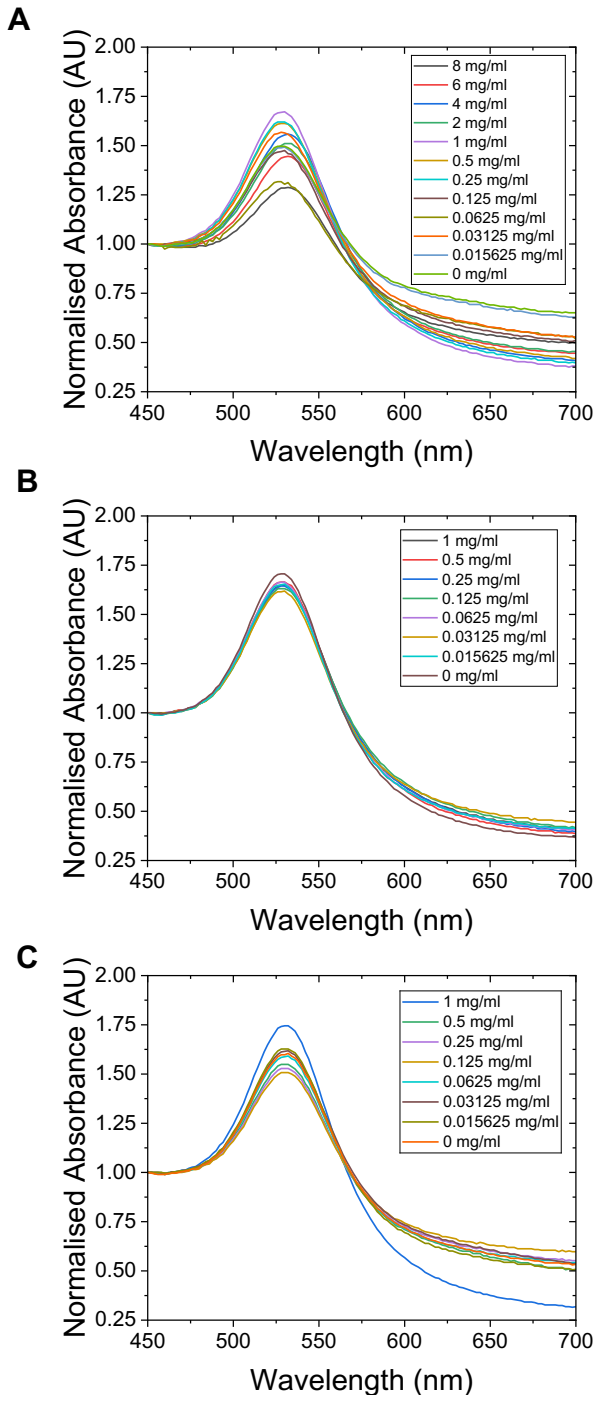

Figure 2. – UV-vis spectra of Gal-2-PHEA42@AuNP40 versus varying concentrations of analyte: A) *C. atrox* venom, B) SBA, and C) WGA Normalised absorbance at 700 nm for Gal-2-PHEA42@AuNP40 nanoparticle system

It is possible that the unexpected lack of binding of certain glycans (especially the terminal Gal residues) to *C. atrox* and SBA may be due to the size of the AuNP or tether chain length. Previous literature has reported that the size of AuNP is crucial to generating a robust signal under certain conditions, with a study by Micallef *I.* demonstrating that 16 nm, 30 nm and, to a lesser extent, 40 nm AuNPs were often too small to signal aggregation, notwithstanding that binding may still occur.[43,63,64] Polymer tether lengths are also well known to impact aggregation outcomes, thus a shorter polymer was utilised along with different-sized, commercially available AuNPs to produce a further library of systems with the Lac-1 and Gal-2 glycans.[43,63,65] This included the inclusion of two new polymers, PHEA$_5$ and PHEA$_{52}$, and AuNP$_{30}$. This synthetic flexibility is a key benefit of a glyco-polymer system versus an antibody system.

The second round of testing was more varied and resulted in the following: Lac-1-pHEA$_{25}$@AuNP$_{30}$ demonstrated no affinity to SBA but displayed strong binding to WGA and a weak affinity to *C. atrox* at higher concentrations, Lac-pHEA$_{25}$@AuNP$_{16}$ displayed little affinity to SBA but strong affinity to both WGA and *C. atrox*, Gal-2-pHEA$_{25}$@AuNP$_{30}$ demonstrated a strong affinity to both WGA and *C. atrox* with no binding exhibited to SBA, Gal-2-pHEA$_{25}$@AuNP$_{16}$ demonstrated moderate affinity to WGA and *C. atrox* along with a weak affinity to SBA, Gal-2-pHEA$_{42}$@AuNP$_{30}$ displayed a moderate affinity to WGA along with a weak affinity to *C. atrox* and SBA. This may offer support that the architecture of SBA requires a larger AuNP to provide a robust signal as noted by Micallef *et al.*.[43] It is also notable that presentation of galactosamine on the polymer via an amide linkage closely mimics GalNAc, a glycan with affinity for WGA.[66]

Partial or full aggregation was again observed by eye, this time with Lac-1-pHEA$_{42}$@AuNP$_{30}$, prior to the plasmonic assay testing indicating an unstable system, likely due to similar reasons as Lac-1-pHEA$_{42}$@AuNP$_{40}$. To explore this further, a final system, Lac-1-pHEA$_{52}$@AuNP$_{16}$ was prepared, to study the effect of a longer polymer tether on the system. The literature suggests that a longer polymer tether should provide increased colloidal stability to the system which it appears to have done. This system did not aggregate immediately and stabilises the 40 nm AuNP, which the shorter polymer tethers were unable to do. Lac-1-pHEA$_{52}$@AuNP$_{40}$ also displayed a strong affinity to WGA and a moderate affinity to *C. atrox,* with no affinity to SBA. Furthermore, comparing Lac-1-pHEA$_{52}$@AuNP$_{40}$ with Lac-1-pHEA$_{52}$@AuNP$_{16}$ indicates that a smaller AuNP is preferable for binding toward *C. atrox*. It was unexpected that a shorter polymer (Lac-1-pHEA$_{25}$@AuNP$_{30}$) allowed the glycosylated nanoparticle system to remain dispersed and did not aggregate like its longer counterpart (Lac-1-pHEA$_{42}$@AuNP$_{30}$). The literature suggests that longer polymers should offer more support to sustain the larger nanoparticles as opposed to shorter polymers.[43,63,65] The data supports the literature in this regard as comparing Lac-1-pHEA$_{42}$@AuNP$_{40}$ and Lac-1-pHEA$_{52}$@AuNP$_{40}$, the former aggregated while the latter remained dispersed. This may indicate that the issue with pHEA$_{42}$ may be due to grafting density and how the polymers chains are 'grafted' onto the AuNP.

To further explore the binding of the nanoparticle library, biolayer interferometry (BLI) studies were carried out using Lac-1-pHEA$_{42}$AuNP$_{16}$, Gal-2-pHEA$_{42}$AuNP$_{40}$, Man-2-pHEA$_{42}$AuNP$_{16}$ and Glc-2-pHEA$_{42}$AuNP$_{16}$ versus *C. atrox* venom and *N. naja* venom (Figure 3.). *N. naja* (Indian cobra) is a snake of the *Elapidae* family, so does not contain lectins compared to *Viperidae*.[39] BLI is an optical biosensing technique that enables the analysis of label-free biomolecular interactions. Multiple protocols were explored including immobilisation of the nanoparticles on the probe, and competition assays. While we saw differences in the binding and dissociation profiles of *C. atrox* and *N. naja* venoms with the particle systems tested, we did not see significant differences between particles with different sugars. Because the venom is a mixture of many components, the binding profile may be dominated by non-specific interactions of proteins other than the lectin of interest.

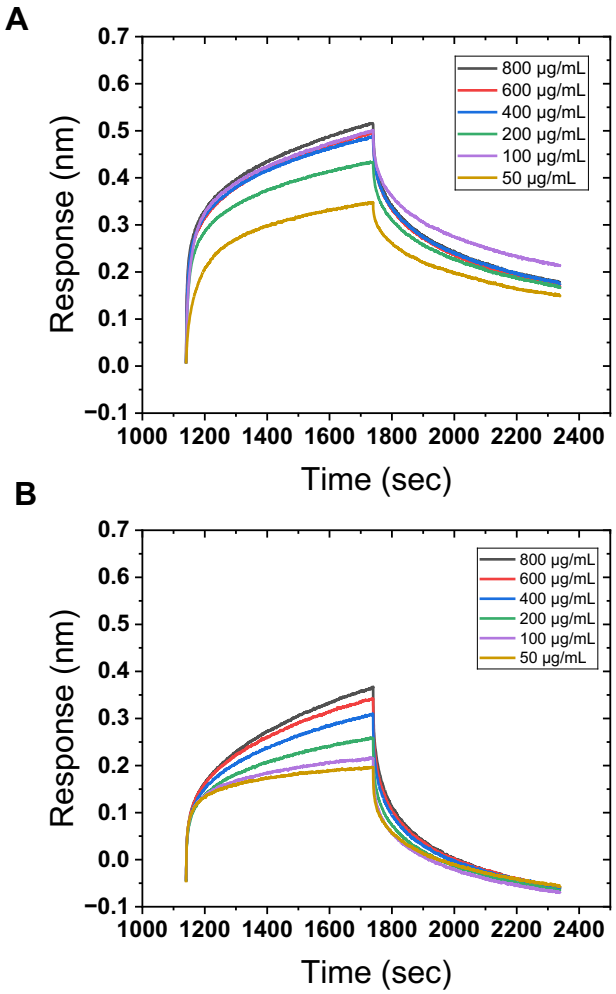

Figure 3. – BLI analysis of Gal-2-PHEA$_{42}$@AuNP$_{40}$ aminopropylsilane sensors versus varying concentrations of analyte: A) *C. atrox* venom, and B) *N. naja* venom

Considering the above, the optimal UV-vis systems, Gal-2-pHEA$_{42}$@AuNP$_{40}$ and Lac-1-pHEA$_{42}$@AuNP$_{16}$, were tested against *N. naja* venom in the UV-vis assay (Figure 4.). UV-vis assays with *N. naja* venom did not show any significant changes as concentration of venom increased again indicating the selectivity of the UV-vis assay for *C. atrox* venom. This is a key advantage of our UV-vis assay approach, that can differentiate *N. naja* venom from *C. atrox* venom despite the multiple components in venoms that impact BLI.

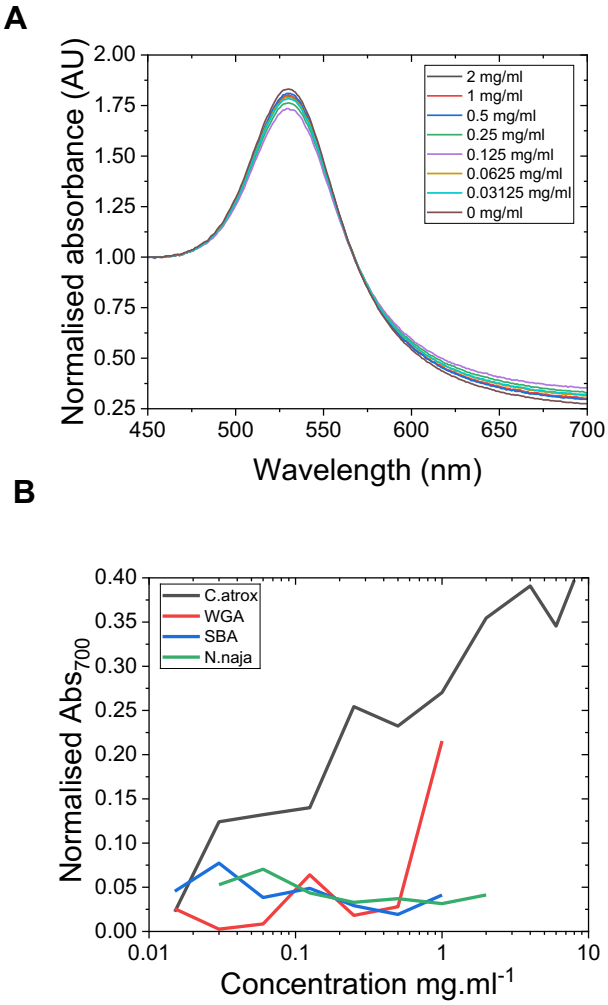

Figure 4. – UV-vis spectra of Gal-2-PHEA$_{42}$@AuNP$_{40}$ versus varying concentrations of *N. naja* venom, and B) Normalised absorbance at 700 nm for Gal-2-PHEA$_{42}$@AuNP$_{40}$ nanoparticle system

Conclusions

In conclusion, a library of glycosylated nanoparticles was synthesised with a range of varying polymer tether lengths, glycans and AuNP sizes. Of which two were successful at rapidly detecting *C. atrox* snake venom specifically and selectively using UV-vis assays against lectin controls, WGA and SBA and a control *Elapidae* venom (*N. naja*). The effect of varying polymer chain length was also studied, with pHEA$_{52}$ polymer being more effective than pHEA$_{42}$ in stabilising larger AuNPs, indicating the importance of careful control of both experimental and chemical parameters to ensure sensitive and specific aggregation.

The optimal systems were Gal-2-pHEA$_{42}$@AuNP$_{40}$ and Lac-1-pHEA$_{42}$@AuNP$_{16}$. Therefore, this study supports the literature that Gal-terminating glycans show affinity to *C. atrox* venom, although purification of RSVL will need to be undertaken to confirm binding to the C-type RSVL. Additionally, comparing the LoD of the Gal-2-pHEA$_{42}$@AuNP$_{40}$ assay to previous literature demonstrates the proof of concept and its future feasibility as a diagnostic tool for *C. atrox* envenomation following further refinement of the glycan. Therefore, this study demonstrates that glycans can be used to sense for snake venom in a prototype UV-vis assay using glycans.

Acknowledgements

The authors would like to thank the following funders. ANB is supported by a Leverhulme Trust Early Career Fellowship (ECF-2023-497). NP was supported by the RSC Undergraduate Summer Bursary Scheme (U24-3487489279). RT is supported by an EPSRC Impact Acceleration Account grant (EP/X525844/1). ML was supported by the Leverhulme Trust (RPG 2019-149 PhD Studentship). AC is supported by a University of Warwick, Department of Chemistry funded PhD.

The Warwick Polymer Research Technology Platform is acknowledged for SEC analysis. The Warwick Polymer and Electron Microscopy Research Technology Platforms are acknowledged for the SEC/EM analysis.

Conflicts of interest

There are no conflicts to declare.

References

(1) Roberts, N. L. S.; Johnson, E. K.; Zeng, S. M.; Hamilton, E. B. *et al.* Global Mortality of Snakebite Envenoming between 1990 and 2019. *Nat Commun* **2022**, *13* (1), 6160.

(2) Pintor, A. F. V.; Ray, N.; Longbottom, J.; Bravo-Vega, C. A.; Yousefi, M.; Murray, K. A.; Ediriweera, D. S.; Diggle, P. J. Addressing the Global Snakebite Crisis with Geo-Spatial Analyses – Recent Advances and Future Direction. *Toxicon X* **2021**, *11*, 100076.

(3) Ratanabanangkoon, K. Merit and Demerit of Polyvalent Snake Antivenoms. *J Toxicol Toxin Rev* **2003**, *22* (1), 77–89.

(4) Isbister, G. K. Antivenom Availability, Delays and Use in Australia. *Toxicon X* **2023**, *17*, 100145.

(5) Isbister, G. The Critical Time Period for Administering Antivenom: Golden Hours and Missed Opportunities. *Clin Toxicol (Phila)* **2024**, 1–3.

(6) Knudsen, C.; Jürgensen, J. A.; Føns, S.; Haack, A. M.; Friis, R. U. W.; Dam, S. H.; Bush, S. P.; White, J.; Laustsen, A. H. Snakebite Envenoming Diagnosis and Diagnostics. *Front Immunol* **2021**, *12*, 661457.

(7) Boldrini-França, J.; Corrêa-Netto, C.; Silva, M. M. S.; Rodrigues, R. S.; de La Torre, P.; Pérez, A.; Soares, A. M.; Zingali, R. B.; Nogueira, R. A.; Rodrigues, V. M.; Sanz, L.; Calvete, J. J. Snake Venomics and Antivenomics of Crotalus Durissus Subspecies from Brazil: Assessment of Geographic Variation and Its Implication on Snakebite Management. *J Proteomics* **2010**, *73* (9), 1758–1776.

(8) Joseph, J. K.; Simpson, I. D.; Menon, N. C. S.; Jose, M. P.; Kulkarni, K. J.; Raghavendra, G. B.; Warrell, D. A. First Authenticated Cases of Life-Threatening Envenoming by the Hump-Nosed Pit Viper (Hypnale Hypnale) in India. *Trans R Soc Trop Med Hyg* **2007**, *101* (1), 85–90.

(9) Dhananjaya, B. L.; Menon, J. C.; Joseph, J. K.; Raveendran, D. K.; Oommen, O. v. Snake Venom Detection Kit (SVDK): Update on Current Aspects and Challenges. In *Clinical Toxinology in Asia Pacific and Africa*; Springer Netherlands: Dordrecht, 2015; pp 379–400.

(10) Williams, D. J.; Faiz, M. A.; Abela-Ridder, B.; Ainsworth, S.; Bulfone, T. C.; Nickerson, A. D.; Habib, A. G.; Junghanss, T.; Fan, H. W.; Turner, M.; Harrison, R. A.; Warrell, D. A. Strategy for a Globally Coordinated Response to a Priority Neglected Tropical Disease: Snakebite Envenoming. *PLoS Negl Trop Dis* **2019**, *13* (2), e0007059.

(11) Kasturiratne, A.; Wickremasinghe, A. R.; de Silva, N.; Gunawardena, N. K.; Pathmeswaran, A.; Premaratna, R.; Savioli, L.; Lalloo, D. G.; de Silva, H. J. The Global Burden of Snakebite: A Literature Analysis and Modelling Based on Regional Estimates of Envenoming and Deaths. *PLoS Med* **2008**, *5* (11), e218.

(12) Gutiérrez, J. M.; Calvete, J. J.; Habib, A. G.; Harrison, R. A.; Williams, D. J.; Warrell, D. A. Snakebite Envenoming. *Nat Rev Dis Primers* **2017**, *3* (1), 17063.

(13) Szymanski, C. M.; Wren, B. W. Protein Glycosylation in Bacterial Mucosal Pathogens. *Nat Rev Microbiol* **2005**, *3* (3), 225–237.

(14) García-Silva, M. T.; Matthijs, G.; Schollen, E.; Cabrera, J. C.; del Pozo, J. S.; Herreros, M. M.; Simón, R.; Maties, M.; Hernández, E. M.; Hennet, T.; Briones, P. Congenital Disorder of Glycosylation (CDG) Type Ie. A New Patient. *J Inherit Metab Dis* **2004**, *27* (5), 591–600.

(15) Yang, A. C.; Ng, B. G.; Moore, S. A.; Rush, J.; Waechter, C. J.; Raymond, K. M.; Willer, T.; Campbell, K. P.; Freeze, H. H.; Mehta, L. Congenital Disorder of Glycosylation Due to DPM1 Mutations Presenting with Dystroglycanopathy-Type Congenital Muscular Dystrophy. *Mol Genet Metab* **2013**, *110* (3), 345–351.

(16) Nozaki, M.; Ohishi, K.; Yamada, N.; Kinoshita, T.; Nagy, A.; Takeda, J. Developmental Abnormalities of Glycosylphosphatidylinositol-Anchor-Deficient Embryos Revealed by Cre/LoxP System. *Lab Invest* **1999**, *79* (3), 293–299.

(17) Orlean, P. Enzymes That Recognize Dolichols Participate in Three Glycosylation Pathways and Are Required for Protein Secretion. *Biochemistry and Cell Biology* **1992**, *70* (6), 438–447.

(18) Maeda, Y.; Tanaka, S.; Hino, J.; Kangawa, K.; Kinoshita, T. Human Dolichol-Phosphate-Mannose Synthase Consists of Three Subunits, DPM1, DPM2 and DPM3. *EMBO J* **2000**, *19* (11), 2475–2482.

(19) Haltiwanger, R. S. Regulation of Signal Transduction by Glycosylation. *Int J Exp Pathol* **2004**, *85* (4), A49–A77.

(20) Bustamante, J. J.; Gonzalez, L.; Carroll, C. A.; Weintraub, S. T.; Aguilar, R. M.; Muñoz, J.; Martinez, A. O.; Haro, L. S. O-Glycosylated 24 KDa Human Growth Hormone Has a Mucin-like Biantennary Disialylated Tetrasaccharide Attached at Thr-60. *Proteomics* **2009**, *9* (13), 3474–3488.

(21) Varki, A.; Kannagi, R.; Toole, B. P. *Glycosylation Changes in Cancer*; Cold Spring Harbor Laboratory Press, 2009.

(22) Yan, Q.; Yao, D.; Wei, L. L.; Huang, Y.; Myers, J.; Zhang, L.; Xin, W.; Shim, J.; Man, Y.; Petryniak, B.; Gerson, S.;

Lowe, J. B.; Zhou, L. O-Fucose Modulates Notch-Controlled Blood Lineage Commitment. *Am J Pathol* **2010**, *176* (6), 2921–2934.
(23) Shental-Bechor, D.; Levy, Y. Folding of Glycoproteins: Toward Understanding the Biophysics of the Glycosylation Code. *Curr Opin Struct Biol* **2009**, *19* (5), 524–533.
(24) Helenius, A.; Aebi, M. Roles of N-Linked Glycans in the Endoplasmic Reticulum. *Annu Rev Biochem* **2004**, *73* (1), 1019–1049.
(25) Marth, J. D.; Grewal, P. K. Mammalian Glycosylation in Immunity. *Nat Rev Immunol* **2008**, *8* (11), 874–887.
(26) Dedola, S.; Ahmadipour, S.; de Andrade, P.; Baker, A. N.; Boshra, A. N.; Chessa, S.; Gibson, M. I.; Hernando, P. J.; Ivanova, I. M.; Lloyd, J. E.; Marín, M. J.; Munro-Clark, A. J.; Pergolizzi, G.; Richards, S.-J.; Ttofi, I.; Wagstaff, B. A.; Field, R. A. Sialic Acids in Infection and Their Potential Use in Detection and Protection against Pathogens. *RSC Chem Biol* **2024**, *5* (3), 167–188.
(27) Neves, M. M. P. S.; Richards, S.-J.; Baker, A. N.; Walker, M.; Georgiou, P. G.; Gibson, M. I. Discrimination between Protein Glycoforms Using Lectin-Functionalised Gold Nanoparticles as Signal Enhancers. *Nanoscale Horiz* **2023**, *8* (3), 377–382.
(28) Baker, A. N.; Hawker-Bond, G. W.; Georgiou, P. G.; Dedola, S.; Field, R. A.; Gibson, M. I. Glycosylated Gold Nanoparticles in Point of Care Diagnostics: From Aggregation to Lateral Flow. *Chem Soc Rev* **2022,** *51*, 7238-7259.
(29) Baker, A. N.; Muguruza, A. R.; Richards, S.; Georgiou, P. G.; Goetz, S.; Walker, M.; Dedola, S.; Field, R. A.; Gibson, M. I. Lateral Flow Glyco-Assays for the Rapid and Low-Cost Detection of Lectins–Polymeric Linkers and Particle Engineering Are Essential for Selectivity and Performance. *Adv Healthc Mater* **2022**, *11* (4), 2101784.
(30) Richards, S.-J. J.; Keenan, T.; Vendeville, J.-B. B.; Wheatley, D. E.; Chidwick, H.; Budhadev, D.; Council, C. E.; Webster, C. S.; Ledru, H.; Baker, A. N.; Walker, M.; Galan, M. C.; Linclau, B.; Fascione, M. A.; Gibson, M. I. Introducing Affinity and Selectivity into Galectin-Targeting Nanoparticles with Fluorinated Glycan Ligands. *Chem Sci* **2021**, *12* (3), 905–910.
(31) Manning, J. C.; Romero, A.; Habermann, F. A.; García Caballero, G.; Kaltner, H.; Gabius, H.-J. Lectins: A Primer for Histochemists and Cell Biologists. *Histochem Cell Biol* **2017**, *147* (2), 199–222.
(32) Ghazarian, H.; Idoni, B.; Oppenheimer, S. B. A Glycobiology Review: Carbohydrates, Lectins and Implications in Cancer Therapeutics. *Acta Histochem* **2011**, *113* (3), 236–247.
(33) Lindberg, A. A.; Brown, J. E.; Strömberg, N.; Westling-Ryd, M.; Schultz, J. E.; Karlsson, K. A. Identification of the Carbohydrate Receptor for Shiga Toxin Produced by Shigella Dysenteriae Type 1. *J Biol Chem* **1987**, *262* (4), 1779–1785.
(34) Richards, R. L.; Moss, J.; Alving, C. R.; Fishman, P. H.; Brady, R. O. Choleragen (Cholera Toxin): A Bacterial Lectin. *Proc Natl Acad Sci U S A* **1979**, *76* (4), 1673–1676.
(35) Li, S. S.; Wei, C. H.; Lin, J.-Y.; Tung, T.-C. Amino-Terminal Sequences of the Anti-Tumor Lectin Ricin A- and B-Chains. *Biochem Biophys Res Commun* **1975**, *65* (4), 1191–1195.
(36) Sartim, M. A.; Sampaio, S. V. Snake Venom Galactoside-Binding Lectins: A Structural and Functional Overview. *J Venom Anim Toxins Incl Trop Dis* **2015**, *21*, 35.
(37) Gartner, T. K.; Stocker, K.; Williams, D. C. Thrombolectin: A Lectin Isolated from *Bothrops Atrox* Venom. *FEBS Lett* **1980**, *117* (1–2), 13–16.
(38) Young, N. M.; van Faassen, H.; Watson, D. C.; Mackenzie, C. R. Specificity Analysis of the C-Type Lectin from Rattlesnake Venom, and Its Selectivity towards Gal- or GalNAc-Terminated Glycoproteins. *Glycoconj J* **2011**, *28* (6), 427–435.
(39) Oliveira, A. L.; Viegas, M. F.; da Silva, S. L.; Soares, A. M.; Ramos, M. J.; Fernandes, P. A. The Chemistry of Snake Venom and Its Medicinal Potential. *Nat Rev Chem* **2022**, *6* (7), 451–469.
(40) Aberasturi, D. J. de; Serrano-Montes, A. B.; Liz-Marzán, L. M. Modern Applications of Plasmonic Nanoparticles: From Energy to Health. *Adv Opt Mater* **2015**, *3* (5), 602–617.
(41) Georgiou, P. G.; Guy, C. S.; Hasan, M.; Ahmad, A.; Richards, S.-J.; Baker, A. N.; Thakkar, N. v.; Walker, M.; Pandey, S.; Anderson, N. R.; Grammatopoulos, D.; Gibson, M. I. Plasmonic Detection of SARS-CoV-2 Spike Protein with Polymer-Stabilized Glycosylated Gold Nanorods. *ACS Macro Lett* **2022**, *11* (3), 317–322.
(42) Richards, S.-J.; Baker, A. N.; Walker, M.; Gibson, M. I. Polymer-Stabilized Sialylated Nanoparticles: Synthesis, Optimization, and Differential Binding to Influenza Hemagglutinins. *Biomacromolecules* **2020**, *21* (4), 1604–1612.
(43) Micallef, J.; Baker, A. N.; Richards, S.-J.; Soutar, D. E.; Georgiou, P. G.; Walker, M.; Gibson, M. I. Polymer-Tethered Glyconanoparticle Colourimetric Biosensors for Lectin Binding: Structural and Experimental Parameters to Ensure a Robust Output. *RSC Adv* **2022**, *12* (51), 33080–33090.
(44) Novogrodsky, A.; Katchalski, E. Transformation of Neuraminidase-Treated Lymphocytes by Soybean Agglutinin. *Proc Natl Acad Sci U S A* **1973**, *70* (9), 2515–2518.
(45) Turner, M. W. The Role of Mannose-Binding Lectin in Health and Disease. *Mol Immunol* **2003**, *40* (7), 423–429.
(46) Schwefel, D.; Maierhofer, C.; Beck, J. G.; Seeberger, S.; Diederichs, K.; Möller, H. M.; Welte, W.; Wittmann, V. Structural Basis of Multivalent Binding to Wheat Germ Agglutinin. *J Am Chem Soc* **2010**, *132* (25), 8704–8719.
(47) Earl, S. T. H.; Robson, J.; Trabi, M.; de Jersey, J.; Masci, P. P.; Lavin, M. F. Characterisation of a Mannose-Binding C-Type Lectin from Oxyuranus Scutellatus Snake Venom. *Biochimie* **2011**, *93* (3), 519–527.
(48) Campa, C.; Donati, I.; Vetere, A.; Gamini, A.; Paoletti, S. Synthesis of Glycosylamines: Indentification and

Quantification of Side Products. *J Carbohydr Chem* **2001**, *20* (3–4), 263–273.

(49) Lubineau, A.; Augé, J.; Drouillat, B. Improved Synthesis of Glycosylamines and a Straightforward Preparation of N-Acylglycosylamines as Carbohydrate-Based Detergents. *Carbohydr Res* **1995**, *266* (2), 211–219.

(50) Lim, D.; Brimble, M. A.; Kowalczyk, R.; Watson, A. J. A.; Fairbanks, A. J. Protecting-Group-Free One-Pot Synthesis of Glycoconjugates Directly from Reducing Sugars. *Angewandte Chemie International Edition* **2014**, *53* (44), 11907–11911.

(51) Hamako, J.; Suzuki, Y.; Hayashi, N.; Kimura, M.; Ozeki, Y.; Hashimoto, K.; Matsui, T. Amino Acid Sequence and Characterization of C-Type Lectin Purified from the Snake Venom of Crotalus Ruber. *Comp Biochem Physiol B Biochem Mol Biol* **2007**, *146* (3), 299–306.

(52) Bastús, N. G.; Comenge, J.; Puntes, V. Kinetically Controlled Seeded Growth Synthesis of Citrate-Stabilized Gold Nanoparticles of up to 200 Nm: Size Focusing versus Ostwald Ripening. *Langmuir* **2011**, *27* (17), 11098–11105.

(53) Calvete, J. J.; Fasoli, E.; Sanz, L.; Boschetti, E.; Righetti, P. G. Exploring the Venom Proteome of the Western Diamondback Rattlesnake, Crotalus Atrox, via Snake Venomics and Combinatorial Peptide Ligand Library Approaches. *J Proteome Res* **2009**, *8* (6).

(54) Otten, L.; Vlachou, D.; Richards, S.-J.; Gibson, M. I. Glycan Heterogeneity on Gold Nanoparticles Increases Lectin Discrimination Capacity in Label-Free Multiplexed Bioassays. *Analyst* **2016**, *141* (14), 4305–4312.

(55) Rao, V. S. R.; Lam, K.; Qasba, P. K. Three Dimensional Structure of the Soybean Agglutinin-Gal/GalNAc Complexes by Homology Modeling. *J Biomol Struct Dyn* **1998**, *15* (5), 853–860.

(56) Frederick, J. R.; Petri, W. A. Roles for the Galactose-/N-Acetylgalactosamine-Binding Lectin of Entamoeba in Parasite Virulence and Differentiation. *Glycobiology* **2005**, *15* (12), 53R-59R.

(57) Maupin, K. A.; Liden, D.; Haab, B. B. The Fine Specificity of Mannose-Binding and Galactose-Binding Lectins Revealed Using Outlier Motif Analysis of Glycan Array Data. **2011**.

(58) Koukalová, T.; Kovaříček, P.; Bojarová, P.; Guerra, V. L. P.; Vrkoslav, V.; Navara, L.; Jirka, I.; Cebecauer, M.; Křen, V.; Kalbáč, M. Reversible Lectin Binding to Glycan-Functionalized Graphene. *Int J Mol Sci* **2021**, *22* (13), 6661.

(59) Cederberg, B. M.; Gray, G. R. N-Acetyl-D-Glucosamine Binding Lectins. A Model System for the Study of Binding Specificity. *Anal Biochem* **1979**, *99* (1), 221–230.

(60) Parasuraman, P.; Murugan, V.; Selvin, J. F. A.; Gromiha, M. M.; Fukui, K.; Veluraja, K. Insights into the Binding Specificity of Wild Type and Mutated Wheat Germ Agglutinin towards Neu5Acα(2-3)Gal: A Study by *in Silico* Mutations and Molecular Dynamics Simulations. *Journal of Molecular Recognition* **2014**, *27* (8), 482–492.

(61) Wangchareansak, T.; Sangma, C.; Ngernmeesri, P.; Thitithanyanont, A.; Lieberzeit, P. A. Self-Assembled Glucosamine Monolayers as Biomimetic Receptors for Detecting WGA Lectin and Influenza Virus with a Quartz Crystal Microbalance. *Anal Bioanal Chem* **2013**, *405* (20), 6471–6478.

(62) Sartim, M. A.; Sampaio, S. V. Snake Venom Galactoside-Binding Lectins: A Structural and Functional Overview. *Journal of Venomous Animals and Toxins including Tropical Diseases* **2015**, *21* (1), 35.

(63) Lión, V.; Rojas, A.; Rodríguez-Acosta, A. Design of an Agglutination Latex Test to Detect Venoms from Viperidae Snakes in Patients' Serum. *Rev Cubana Med Trop* **2004**.

(64) Georgiou, P. G.; Baker, A. N.; Richards, S.-J. J.; Laezza, A.; Walker, M.; Gibson, M. I. "Tuning Aggregative versus Non-Aggregative Lectin Binding with Glycosylated Nanoparticles by the Nature of the Polymer Ligand." *J Mater Chem B* **2020**, *8* (1), 136–145.

(65) Pancaro, A.; Szymonik, M.; Georgiou, P. G.; Baker, A. N.; Walker, M.; Adriaensens, P.; Hendrix, J.; Gibson, M. I.; Nelissen, I. The Polymeric Glyco-Linker Controls the Signal Outputs for Plasmonic Gold Nanorod Biosensors Due to Biocorona Formation. *Nanoscale* **2021**, *13* (24), 10837–10848.

(66) Baker, A. N.; Hawker-Bond, G. W.; Georgiou, P. G.; Dedola, S.; Field, R. A.; Gibson, M. I. Glycosylated Gold Nanoparticles in Point of Care Diagnostics: From Aggregation to Lateral Flow. *Chem Soc Rev* **2022**, *51* (16), 7238–7259.

(67) Peters, B. P.; Goldstein, I. J.; Flashner, M.; Ebisu, S. Interaction of Wheat Germ Agglutinin with Sialic Acid†. *Biochemistry* **1979**, *18* (24).